

### **Appendix: The Hertz contact theory**

The Hertz contact theory consists of a series of mathematical equations to calculate normal, hoop, radial, and shear stress components on and within a soft flat surface or half-space, known as the specimen, when pressed by a rigid hemisphere called the indenter (**Appendix Figure 1**) [1]. We have employed this theory in order to calculate stresses within muscle tissue when pressed by the ischial tuberosities (IT). The Hertz theory is based on a number of assumptions that are not necessarily in line with the physical reality of the buttocks geometry and must be accounted for when considering the results of the present application of the Hertz model [2–3]. The foremost of these assumptions are that the half-space is infinite and the deformations into it are relatively small, that both surfaces are ideally smooth (no friction between them), and that the materials are homogeneous, isotropic, and elastic. The first assumption stands in contrast to the anatomy of the IT and gluteus—the muscle is not an infinite half-space tolerating small indentations but a finite-thickness tissue enduring large deformations. In order to compensate for this assumption and take the large deformation mechanics into account, we employed a correction factor  $\alpha$  (**Appendix Figure 2**), projecting the Zhang et al. study [4] to a 25% indentation of the tissue [5]. The second assumption disagrees with the fact that the IT and the gluteus are physically connected and therefore not only is friction a fundamental part of their interaction but practically there is no such thing as a “contact patch”—a radius outside of which there is no contact between the bodies according to the Hertz model. The third assumption implies that the muscle will probably behave, mechanically, in a more complex manner than we presume in the model. Still, the contradiction between assumptions and physical reality influences mostly the stress components of tension and shear, which, on initial examination, were found to be too remote from the well-established values of finite element (FE) models and were therefore excluded from the scope of this study. Nevertheless, keeping a comprehensive and futuristic view in mind, the model and system were developed for the whole range of stress components.

The following parameters serve the equations

$$G_{it} = \frac{E_{it}}{2(1+\nu_{it})} \quad ; \quad G_{st} = \frac{\alpha E_{st}}{2(1+\nu_{st})} \quad \text{and} \quad (\text{A1a;A1b})$$

$$A = \frac{1-\nu_{it}}{G_{it}} + \frac{1-\nu_{st}}{G_{st}}, \quad (\text{A2})$$

where  $G_{it}$ ,  $G_{st}$  are the shear modulus of IT and muscle tissue, respectively,  $\nu_{it}$ ,  $\nu_{st}$  are their Poisson's ratios,  $E_{it}$ ,  $E_{st}$  are the elastic moduli, and  $\alpha$  is the correction factor for large deformations in the tissue. Zhang et al. [4] carried out studies on a FE model to determine  $\alpha$  (termed  $\kappa$  in their paper) by indenting a tissue layer at 0.1, 10, and 15% of its original finite thickness ( $h$ ). This was performed for a series of ratios between the indenter radii ( $a$ ) to the original thickness ( $h$ ). We projected these values linearly to determine a series of  $\alpha$ -s at the indentation of 25% (**Appendix Figure 2**). A second degree polynomial was fitted to this series in order to calculate  $\alpha$  for a subject's IT radius over soft tissue thickness ratio (**Appendix Figure 3**).

$k$ , the curvature is defined as

$$k = \frac{1}{R_{it}} + \frac{1}{R_{st}}, \quad (\text{A3})$$

where  $R_{it}$ ,  $R_{st}$  are the radii of IT and muscle soft tissue, respectively.  $R_{st}$  is considered infinite for a half-space. A time-dependent contact patch radius,  $a(t)$ , is calculated by

$$a(t) = \sqrt[3]{\frac{3F(t)A}{8k}}, \quad (\text{A4})$$

where  $F(t)$  is the time-dependent compressive force transferred through the IT due to body weight (measured herein in real-time by integration of interface pressures over the buttocks-support contact area under the IT).

A geometric parameter  $u(t)$ , for a specific point in the tissue, is given by

$$u(t) = 0.5 \left[ r^2 + z^2 - a(t)^2 \pm \sqrt{(r^2 + z^2 - a(t)^2)^2 + 4a(t)^2 z^2} \right], \quad (\text{A5})$$

where  $r$  is the radius from the origin, that is, the center of bone-muscle contact, and  $z$  is the depth into the tissue.

The time-dependent peak bone-muscle contact (compression) stress  $P_0(t)$ , is

$$P_0(t) = \frac{3F(t)}{2\pi a(t)^2}, \quad (\text{A6})$$

and the time-dependent internal compression stress distribution in the muscle is

$$\sigma_{zz}(t) = P_0(t) \left( \frac{z}{\sqrt{u(t)}} \right)^3 \frac{a(t)^2 u(t)}{u(t)^2 + a(t)^2 z^2}. \quad (\text{A7})$$

The axes where  $r=0$  and  $z=0$  are special cases where the equations are simplified. Specifically, when  $r=0$

$$\sigma_{zz}(t) = P_0(t) \frac{a(t)^2}{a(t)^2 + z^2}, \quad (\text{A8})$$

and when  $z=0$  and  $r < a$

$$\sigma_{zz}(t) = P_0(t) \frac{\sqrt{a(t)^2 - r^2}}{a(t)}. \quad (\text{A9})$$

At the origin ( $r=0, z=0$ )

$$\sigma_{zz}(t) = P_0(t), \quad (\text{A10})$$

and when  $z=0$  and  $r \geq a$

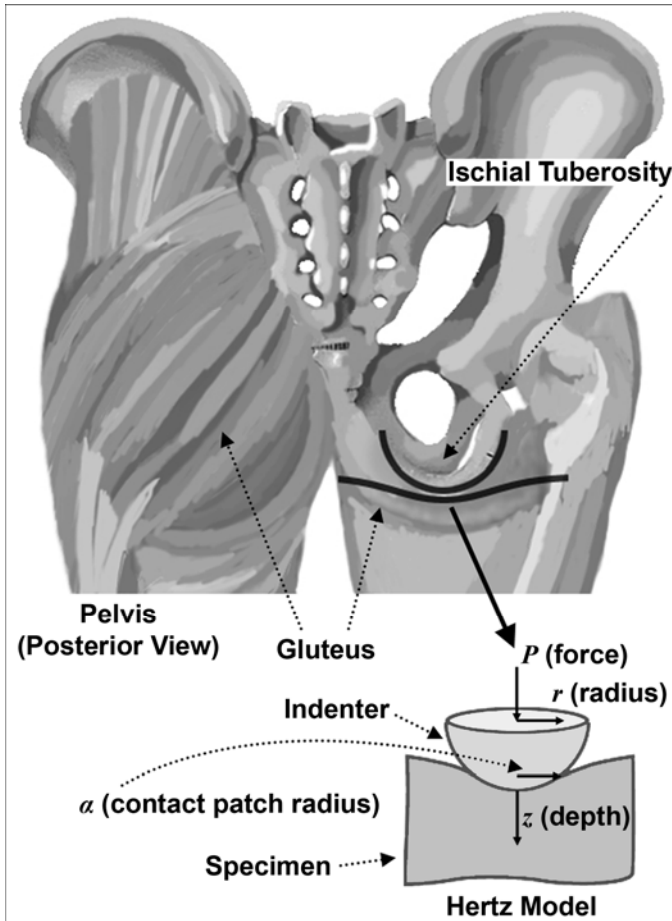
$$\sigma_{zz} = 0. \quad (\text{A11})$$

In order to depict the individual influences of the model parameters on the measure outcome of peak muscle compression stress  $P_0(t)$ , we conducted a sensitivity analysis. Specifically, we determined the relative sensitivity of peak muscle compression stress calculations to changes in

the model parameters, namely, the elastic modulus of muscle tissue, the force transferred through the ischial tuberosity (IT) which depends on the body posture and is measured in real-time, and the radius of curvature of the IT (**Appendix Figure 4**). The results of this analysis revealed that in the physiologically-reasonable range of parameter variation, i.e. coefficient of change in model parameters in the order of up to 2-3 [6–7] variations in muscle stiffness and IT radius of curvature appear to affect peak compression stresses in muscle to a similar extent (though in opposite trends). For (theoretical) greater parameter variations, the reduction in peak muscle stress with the increasing IT radius becomes asymptotic, whereas further increase in muscle tissue stiffness has a more monotonic effect on increasing peak muscle stress (**Appendix Figure 4**). A more comprehensive sensitivity analysis of this model that also considers the presence and time-course of development of deep tissue injury, and its potential effects on the stress state in muscle tissue under the IT, is provided elsewhere [2].

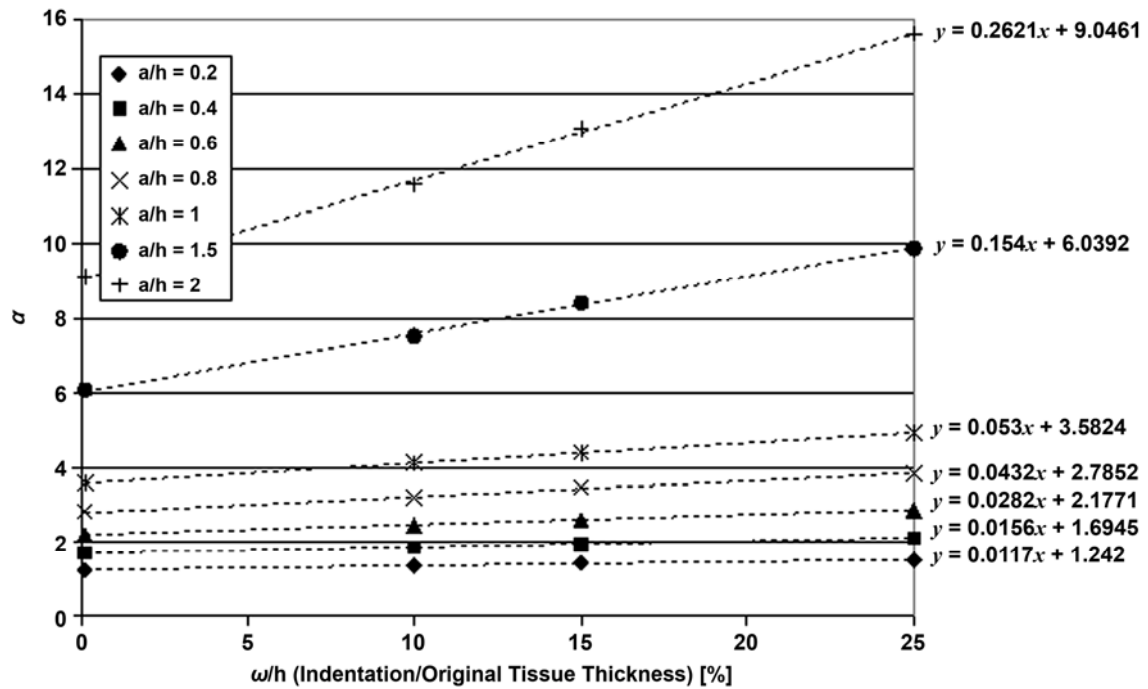
**Appendix Figure 1.**

Classical Hertz sphere-half space contact model as simplified representation of ischial tuberosities and gluteus.



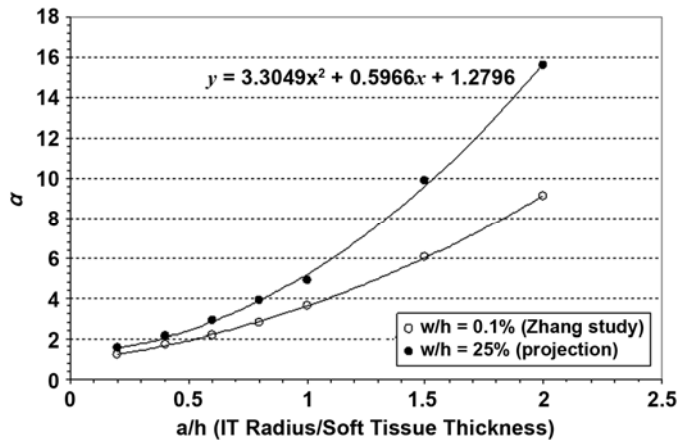
**Appendix Figure 2.**

Linear projections of Zhang et al. study [4]. Each series of  $\alpha$  values for  $a/h$  ratio ( $a$  = ischial tuberosity radius,  $h$  = muscle tissue thickness) was projected linearly to indentation/original tissue thickness ratio of 25 percent. Linear equations used are shown by each trend line.



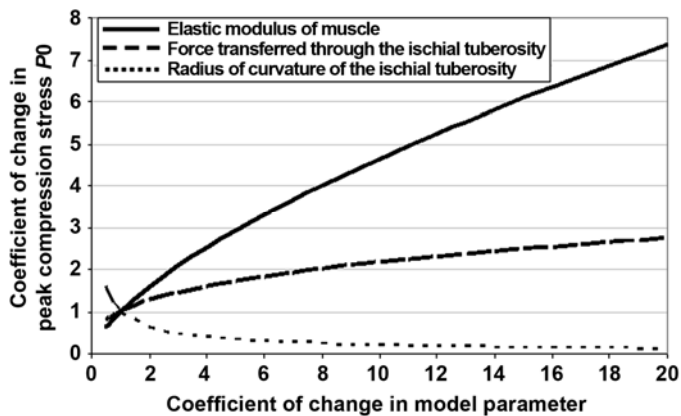
**Appendix Figure 3.**

Polynomial for calculation of correction factor  $\alpha$ , given subject's muscle tissue thickness and ischial tuberosity radius. Our projection for indentation of 25 percent is shown, along with original data adopted from Zhang [4].



**Appendix Figure 4**

Analysis of sensitivity of peak muscle compression stress calculations to changes in model parameters, namely, elastic modulus of muscle tissue, force transferred through ischial tuberosity (IT) (which depends on body posture and is measured in real-time), and radius of curvature of IT.



## References

1. Huber MT. Zur theorie der berührung fester elastischer körper. Annalen der Physik. 1904;14:153–63.
2. Gefen A. Risk factors for a pressure-related deep tissue injury: A theoretical model. Med Biol Eng Comput. 2007;45(6):563–73. [[PMID: 17486382](#)]
3. Deeg EW. New algorithms for calculating Hertzian stresses, deformations, and contact zone parameters. AMP J Technol. 1992;2:14–24.
4. Zhang M, Zheng YP, Mak AF. Estimating the effective Young's modulus of soft tissues from indentation tests—Nonlinear finite element analysis of effects of friction and large deformation. Med Eng Phys. 1997;19(6):512–17. [[PMID: 9394898](#)]
5. Oomens CW, Bressers OF, Bosboom EM, Bouten CV, Blader DL. Can loaded interface characteristics influence strain distributions in muscle adjacent to bony prominences? Comput Methods Biomech Biomed Engin. 2003;6(3):171–80. [[PMID: 12888429](#)]
6. Linder-Ganz E, Shabshin N, Itzchak Y, Gefen A. Assessment of mechanical conditions in sub-dermal tissues during sitting: A combined experimental-MRI and finite element approach. J Biomech. 2007;40(7):1443–54. [[PMID: 16920122](#)]
7. Palevski A, Glaich I, Portnoy S, Linder-Ganz E, Gefen A. Stress relaxation of porcine gluteus muscle subjected to sudden transverse deformation as related to pressure sore modeling. J Biomech Eng. 2006;128(5):782–87. [[PMID: 16995767](#)]